DETECTION OF MICROCALCIFICATIONS USING NON-LINEAR FILTERING

Dirk Meersman, Paul Scheunders, Dirk Van Dyck
VisionLab, Dept. of Physics,
RUCA, University of Antwerp,
Groenenborgerlaan 171,
2020 Antwerp, BELGIUM
Tel: +32 3 218.04.39; fax: +32 3 218.03.18
e-mail: Dirk.Meersman@ruca.ua.ac.be

ABSTRACT

In this paper we describe a microcalcification detection scheme using non-linear filtering. Our scheme uses a combination of two highly non-linear filters: one for image enhancement, and one for the actual detection of the microcalcifications. Results of our method on the Nijmegen mammographic image database are given.

1 INTRODUCTION

Nowadays, breast cancer is an important cause of death for women. With current state-of-the-art techniques in the field of breast cancer treatment, early detection seems to be a crucial factor for the success of the treatment. The presence of microcalcifications in mammographic images is a important feature in the early detection of breast cancer. These microcalcifications are present in the images as small regions (0.1 - 1.0 mm ø) with an intensity slightly brighter than the surrounding breast tissue. Due to these properties, a human observer sometimes fails to detect clusters of microcalcifications. In the near future, Computer Aided Diagnosis (CAD) systems can be used as diagnostic tools to avoid these errors. The work presented here is part of the development of a CAD-system for the automated detection of microcalcifications in mammograms. Previous work in the field showed that neural networks are capable of detecting microcalcifications in mammograms [2, 6, 7, 11, 12, 14]. This work also showed that the usage of neural networks can involve large computational efforts due to the size of the mammographic images (2k x 2k or more). The aim of our method was to restrict the amount of data to be processed to a small number of regions in each image, without losing the detectability of the present clusters of microcalcifications.

2 MATERIALS

2.1 Dataset

For the development of the microcalcification detection scheme, we used a public domain mammographic image database [1]. This set has been used by several other researchers [4, 5, 10, 11, 13]. It consists out of 40 mammograms, digitized using a 12 bit CCD camera with a 0.05 mm sampling aperture and 0.1 mm sampling distance. The dataset contains 105 clusters of microcalcifications, including benign and malignant cases. Each image in the set has a size of 2048^2 pixels. Truth information about the size and position of the contained clusters of microcalcifications is given by a series of circular regions marked by radiologists.

2.2 Evaluation of performance

The construction of a ROC-curve (Receiver Operating Characteristic) is, in the medical world, a standard way for evaluating the diagnostic performance of a test [8, 15]. For the construction of these curves, the problem of diagnosis is considered as a two-class problem: one class of the population having a certain disease, the second, not having this disease. For each test, a number of cases of the first class will be correctly classified as positive (TP, true positive), and a number of cases of this class will be wrongly classified negative (FN, false negative). The same is true for the second class, giving false positives (FP) and true negative (TN) cases. Depending on the criterion used (e.g. a threshold on a measured value) in the test, these numbers will change. A ROC-curve is a graphical representation of the TP-rate versus the FP-rate for different values of the criterion. If, for a certain test, a single member of the population can have multiple results (e.g. a mammographic image that contains either two separated TP regions or one TP and one FP region), the measurement of the FP-rate becomes impossible. The FP-rate per image can be used instead. The resulting curve is called a FROC-curve (Free response ROC). We refer to [9] for a more in depth overview of the use of ROC and FROC analysis in digital mammography.

3 MICROCALCIFICATION DETECTION SCHEME

3.1 Preprocessing Stage

The first stage in our microcalcification detection scheme is a preprocessing step to remove the background tissue structures from the images. For this purpose, we have applied a median-subtraction step. After analyzing

the results of this step, we decided that a second correction step was necessary to normalize for the variations in the local gray level distributions of the images.

3.1.1 Background subtraction

Because of its edge preserving properties and its simplicity in implementation, we have used a localized median filter to fit the background tissue. The size of the local region for the calculation of the median was chosen to be about twice the size of the larger microcalcifications present in the images (2 mm ø). In this way, the result image contains a maximal amount of background tissue variations, without containing the smaller objects such as noise, small edges and microcalcifications. By subtracting this filtered result from the original image, we obtain an image containing only these small particles.

3.1.2 Normalization

After the removal of the background tissue, we noticed that the distribution of the regions with high intensity values was not equal over the entire images. Especially in regions with low intensity (e.g. near the edges of the breast), we detected a much lower density of regions with high intensity. To compensate for this, we measured the local variance in the images and applied:

$$I'(x,y) = \frac{I(x,y)}{\sqrt{1+\sigma^2(x,y)}} \tag{1}$$

with:

$I'(x,y)$	:	the new pixel value
$I(x,y)$	:	the original greyvalue at point (x,y)
$\sigma^2(x,y)$	:	the local variance of (x,y)

The result of this normalization is an image with a much more equally spread distribution of regions with high intensity values.

3.2 Signal Enhancement

In this step we use a non-linear filter (extremum filter [3]) for the removal of the image noise and to enhance the microcalcification-like shapes present in the images. An extremum filter is a type of filter that looks for dome-shaped objects in the image and reduces the noise. The filter replaces each point (x,y) by the extremum value of the quadratic function $F(x,y) = a_1x^2 + a_2y^2 + a_3xy + a_4x + a_5y + a_6$ fitted to the point's local neighborhood. In this way, if a pixel is part of a dome-shaped object, the fitted function will have a large maximum value, giving a high output value. If, on the other hand, the pixel is a part of the background or a region containing a lot of noise, the fitted function will be flatter, giving a smaller extremum value and a lower output. An overview of the behavior of the output of the extremum filter is given below:

$$Out(x,y) = \begin{cases} high & \text{if } (x,y) \in \text{gaussian-shaped object} \\ low & \text{if } (x,y) \in \text{backgound} \\ low & \text{if } (x,y) \in \text{noise} \end{cases} \tag{2}$$

Since microcalcifications can be considered dome-shaped objects an extremum filter can be used to enhance them. In our application we set the windowsize for the calculation of the quadratic form to five by five pixels. The output image shows an increased visibility of the microcalcifications and a reduced noise level.

3.3 Detection stage

For the detection of microcalcifications, we used their property of having higher intensity distributions compared to the surrounding background. If we consider the normal intensity distributions in the (pre-processed) local background, the intensity of pixels belonging to microcalcifications can be seen as outliers to this distribution. The boxplot detection method, a standard outlier detection scheme, can be used for their detection:

$$I'(x,y) = \begin{cases} 1 & \text{if } I(x,y) < P_{25} + \alpha \cdot (P_{75} - P_{25}) \\ 1 & \text{if } I(x,y) > P_{75} + \alpha \cdot (P_{75} - P_{25}) \\ 0 & \text{elsewhere} \end{cases} \tag{3}$$

with :

$I'(x,y)$	:	output value (1=outlier,0=no outlier)
$I(x,y)$	:	the original pixel value
α	:	a constant
P_{xx}	:	the local percentile value (xx=25,75)

A problem in the application of this scheme is the proper choice of the value for α (usual 1.5 or 3). The output of this boxplot outlier detection scheme is binary, being 1 if the value of a point exceeds the calculated value or 0 if it doesn't. We adapted this idea to create a filter of which the output would be a measure for the outlying of a point. We did this by solving the second line in the boxplot equation (3) for the constant α giving the equation below.

$$\alpha(x,y) = \frac{I(x,y) - P_{75}}{(P_{75} - P_{25})} \tag{4}$$

At each point in the image we replaced the point's original value $I(x,y)$ by the calculated α-value ($\alpha(x,y)$). In this way the output value of this filter at a point (x,y) is a measure for the variation from the 'normal' distribution of greyvalues of the local image region. For our application, we used a large local region (about 1cm x 1cm) around the pixel to calculate the values of P_{25} and P_{75}, allowing the values of P_{25} and P_{75} to adapt to the local properties of the pixel's neighborhood.

4 Results

The different stages in the detection scheme are shown in Figure 1 where the scheme was applied to a region

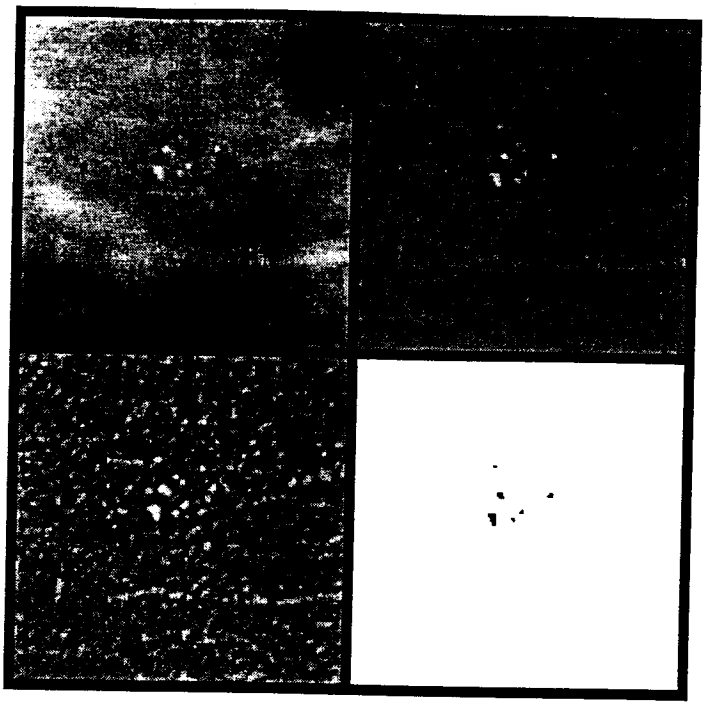

Figure 1: Illustration of the various stages in the detection scheme: the original image data (upper left), the image after preprocessing (upper right), the enhanced image (lower left) and the detected regions obtained by thresholding the enhanced image (lower right).

containing a cluster of microcalcifications: the original image data (upper left), the preprocessed image data (upper right), the output of the percentile filter (lower left) and the detected regions (lower right). These images were enhanced for an improved visibility.

By thresholding the resulting image at different values, a FROC-curve was constructed (Figure 2). As shown in this figure, our method is able to correctly identify 90% of the clusters of microcalcifications with about 2.5 false positive detected clusters per image. This ratio is higher than the results reported by others on the same dataset [4, 10, 11]. However, for our application, the reduction of the searchspace in the images is more important than the quality of the FROC-curve. By a proper choice of a threshold value, we are ,with this technique, able to reduce the searchspace form the $\pm 10^6$ pixels contained in the image data to $\pm$ 200 regions per image while we maintain the ability to detect 99 % of the clusters of microcalcifications present in the image set. In a next step, we will use these results to construct a feature based classifier for the extraction of the microcalcifications from this set of detected regions.

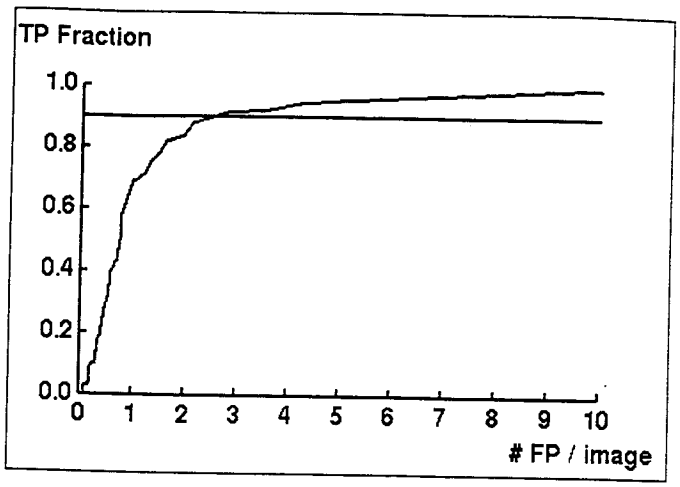

Figure 2: Resulting FROC-curve of the detection scheme. The horizontal line illustrates where the curve reaches the 90% TP-fraction detection rate.

References

[1] Images were provided by courtesy of the national expert and training centre for breast cancer and the departement of radiology at the university of nijmegen, the netherlands.

[2] H. Chan, S. Lo, B. Sahiner, K. Lam, and M. Helvie. Computer-aided detection of mammographic microcalcifications: Pattern recognition with an artificial neural network. *Medical Physics*, 22(10):1555–1567, 1995.

[3] J.-M. Dinten, M. Darboux, and E. Nicolas. A global approach for localization and characterisation of microcalcifications in mammograms. *Digital Mammography '96*, pages 235–238, 1996.

[4] N. Karssemeijer. Adaptive noise equalisation and recognition of microcalcifications clusters in mammograms. *International Journal of Pattern Recognition and Artificial Intelligence*, 7:1357–1376, 1993.

[5] W. Kegelmeyer. Dense feature maps for detection of calcifications. *Digital mammography*, pages 13–20, 1994.

[6] S. Lo, H. Chan, J. Lin, H. Lai, M. Freedman, and S. Mum. Artificial convolution neural network for medical image pattern recognition. *Neural Networks*, 8:1–14, 1995.

[7] D. Meersman, P. Scheunders, and D. V. Dyck. Detection of microcalcifications using neural networks. *Digital Mammography '96*, pages 287–291, 1996.

[8] C. Metz. Basic principles of roc analysis. *Seminars in Nucleair Medicine*, 148:283–843, 1978.

[9] C. Metz. Evaluation of digital mammography by roc analysis. *Digital Mammography '96*, pages 61–68, 1996.

[10] T. Netsch. A scale-space approach for the detection of clustered microcalcifications in digital mammograms. *Digital mammography '96*, pages 301–306, 1996.

[11] D. Rosenthal. Cancer therapy – the 21st century. *CA: A Cancer Journal for Clinicians*, 46(3):131–133, 1996.

[12] B. Sahiner, H.-P. Chan, N. Pertick, D. Wei, M. Helvie, D. Adler, and M. Goodsitt. Image classifications using artificial neural networks. *SPIE*, 2434:838–845, 1995.

[13] R. Strickland and H. Hahn. Wavelet transform for detecting microcalcifications in mammography. In *Proc. ICIP'94*, pages 402–406, 1994.

[14] W. Zang, K. Doi, M. Giger, Y. Wu, R. Nishikawa, and R. Schmidt. Computerized detection of clustered microcalcifications in digital mammograms using a shift-invariant artificial neural network. *Medical Physics*, 21:517–524, 1994.

[15] M. Zweig and G. Cambell. Receiver-operating characteristic (roc) plots: a fundamental evaluation tool in clinical medicine. *Clinical Medicine*, 39:561–577, 1993.